Microbial Physiology

Research Article

Microbial Physiol 2025;35:87–100
DOI: 10.1159/000548185

Received: July 28, 2025
Accepted: August 18, 2025
Published online: August 28, 2025

A FocA Variant Incapable of Formate Import but Retaining Formic Acid Efflux Highlights the Distinct Mechanisms Governing Bidirectional Formate Translocation

Michelle Kammel[a] Oliver Trebbin[a, b] R. Gary Sawers[a]

[a]Institute for Biology/Microbiology, Martin-Luther University Halle-Wittenberg, Halle (Saale), Germany; [b]IMD Laboratory Oderland GmbH, Frankfurt, Germany

Keywords
Formic acid · Formate channel · Formate hydrogenlyase · Formate translocation · $FocA_{H209C}$ mutant

Abstract

Introduction: FocA belongs to the formate-nitrite transporter superfamily of pentameric membrane proteins, which translocate small, monovalent anions across the cytoplasmic membrane of bacteria, archaea, and certain protists. FocA translocates formate anions or formic acid bidirectionally through a hydrophobic pore present in each protomer. This pore has two highly conserved amino acid residues, threonine-91 and histidine-209, that are proposed to protonate the anion during the translocation process. Current evidence suggests that different mechanisms control efflux and influx of formate. ***Methods:*** Determination of changes in extracellular and intracellular formate levels was used to characterize new amino acid variants of FocA in which H209 was exchanged for cysteine or serine. ***Results:*** While the $FocA_{H209S}$ mutant excreted formic acid very efficiently, the mutant synthesizing $FocA_{H209C}$ translocated formic acid out of the cell poorly. These different efflux efficiencies of formic acid through FocA clearly suggest that the reactivity of the sulfur atom in cysteine accounts for the inefficient translocation of formic acid by the $FocA_{H209C}$ variant. Mutants synthesizing the $FocA_{H209S}$ or $FocA_{H209C}$ variants were incapable to importing formate, or its toxic chemical analog hypophosphite, a phenotype similar to previously identified H209-exchange variants. Notably, a mutant lacking a functional formate hydrogenlyase-1 (FHL-1) complex, which under physiological conditions disproportionates formate to H_2 and CO_2, retained sensitivity to hypophosphite but accumulated formate externally. ***Conclusions:*** Our findings indicate that, while coupling between FocA and FHL-1 controls formate import, the import of hypophosphite is not dependent on FHL-1. Further, our data support a model in which two mechanisms for formate import exist, depending on the external formate concentration: at low concentration, protonation of formate or hypophosphite by H209 facilitates anion translocation; at high concentration, formic acid is directed to FHL-1 where it is disproportionated to H_2 and CO_2.

Plain language summary

Ion channels and active transporters are essential for regulation of pH, ion homeostasis, and nutrient acquisition. Generally, the flux of molecules across biological membranes is tightly controlled, and translocation rates, specificity, and further factors (e.g., dependence on gradients or interacting

karger@karger.com
www.karger.com/mip

Correspondence to:
R. Gary Sawers, gary.sawers@mikrobiologie.uni-halle.de

proteins) differ and are constrained by the protein's classification. Here, we investigate the *Escherichia coli* formate channel, FocA, a central channel, which is functional during mixed-acid fermentation and is important for formate and pH homeostasis. FocA translocates formate or formic acid bidirectionally, apparently using a channel-type mechanism in the efflux direction and a transport mechanism for uptake. Here, we identify and characterize a novel translocation variant, in which efflux follows ion channel behavior, but where influx is impaired.

Introduction

In contrast to lactate, acetate, succinate, and ethanol, formate is the only mixed-acid fermentation product that is reimported when cultures of enterobacteria attain an acidic pH, usually upon entry into the stationary phase [1, 2]. Cells reimport formic acid to offset acidification of their immediate environment, and they disproportionate it to the gaseous products H_2 and CO_2, a reaction catalyzed by the membrane-associated and cytoplasmically oriented formate hydrogenlyase-1 (FHL-1) complex [3–5]. Synthesis of FHL-1 is induced when the intracellular formate concentration during fermentation reaches near-mM levels [6]. Formate is sensed by the formate hydrogenlyase activator, FhlA, a transcription factor that, when bound by formate, activates expression of the formate regulon [7]. This regulon comprises genes whose products include the structural components of FHL-1, as well as those of enzymes necessary for synthesis of the heterometallic nickel-iron cofactor of [NiFe] hydrogenases [7–9]. The FHL-1 complex comprises two cytoplasmically oriented catalytic components, namely, hydrogenase-3 and formate dehydrogenase FDH-H, the former being encoded by the *hycA-I* operon and the latter by the *fdhF* gene [4, 10].

Formate is generated during fermentation as a product of the coenzyme A-dependent cleavage of pyruvate by the anaerobically inducible pyruvate formate-lyase (PflB) enzyme, with the other product of the reaction being acetyl-coenzyme A [11]. PflB is encoded in the bicistronic *focA-pflB* operon, which also includes the gene encoding the pentameric transmembrane protein, FocA [12, 13]. FocA belongs to the meanwhile large formate-nitrite transporter superfamily and functions in the bidirectional translocation of formic acid across the membrane [2]. During fermentative growth with glucose, formate begins to accumulate and is sensed by FhlA, which in turn induces synthesis of the FHL-1 complex. Formate can then be either disproportionated by FHL-1, or translocated out of the cell together with a proton, as formic acid [14]. Once the external pH begins to decrease below 7, which occurs upon accumulation of mixed acid fermentation products, formic acid, or possibly formate [2, 14], is then reimported into the cells, where it is disproportionated. Importantly, import of formate or formic acid does not occur in mutants unable to generate an active FHL-1 complex [15], suggesting direct or indirect coupling between FocA-dependent formate uptake and FHL-1 activity. The importance of the combined functions of FocA and FHL-1 in disproportionating formic acid for the fermenting cell may include maintenance of pH homeostasis, or they may conceivably make a contribution to energy conservation in stationary-phase cells [5, 16].

As well as formate-nitrite transporter proteins sharing conserved quaternary structures [17–20], some of the amino acid residues within the hydrophobic translocation pore are also conserved [17, 21]. This is particularly true for the highly conserved histidine (H209 in *Escherichia coli* numbering) and T91 residues, with the former representing the only charged residue within the central portion of the hydrophobic pore (shown in Fig. 1). T91 is able to form a hydrogen bond with H209 [18, 22] (shown in Fig. 2a), which is considered to be important during the translocation of formate or formic acid through FocA's pore [2, 21]. Recent mutational studies, which reported on changes in intracellular formate levels in mutants synthesizing FocA variants, and which were monitored using a chromosomally encoded formate-responsive reporter system, have demonstrated that both residues play an essential role in import of formate or formic acid by FocA [21, 23, 24]. In the efflux direction, only T91 (or a serine substitution variant) allows formic acid translocation by FocA to occur [21], while H209 can be replaced by certain small, neutral residues [21, 23]. However, these latter FocA variants exhibit an efflux-only phenotype, whereby formic acid is very efficiently excreted from the cells. Indeed, formic acid efflux by such $FocA_{H209}$ variants is so efficient that intracellular formate levels are insufficient to induce synthesis of the FHL-1 complex [23]. Amino acid residue exchanges of H209 in FocA that result in this efflux-only phenotype include alanine, asparagine, threonine, and isoleucine [21]. However, substitution of H209 with charged (Asp or Lys) or bulky (Trp or Phe) residues generates FocA variants that fail to translocate formic acid efficiently out of the cells; thus, formate anions accumulate intracellularly. These FocA variants can nevertheless import some exogenously supplied

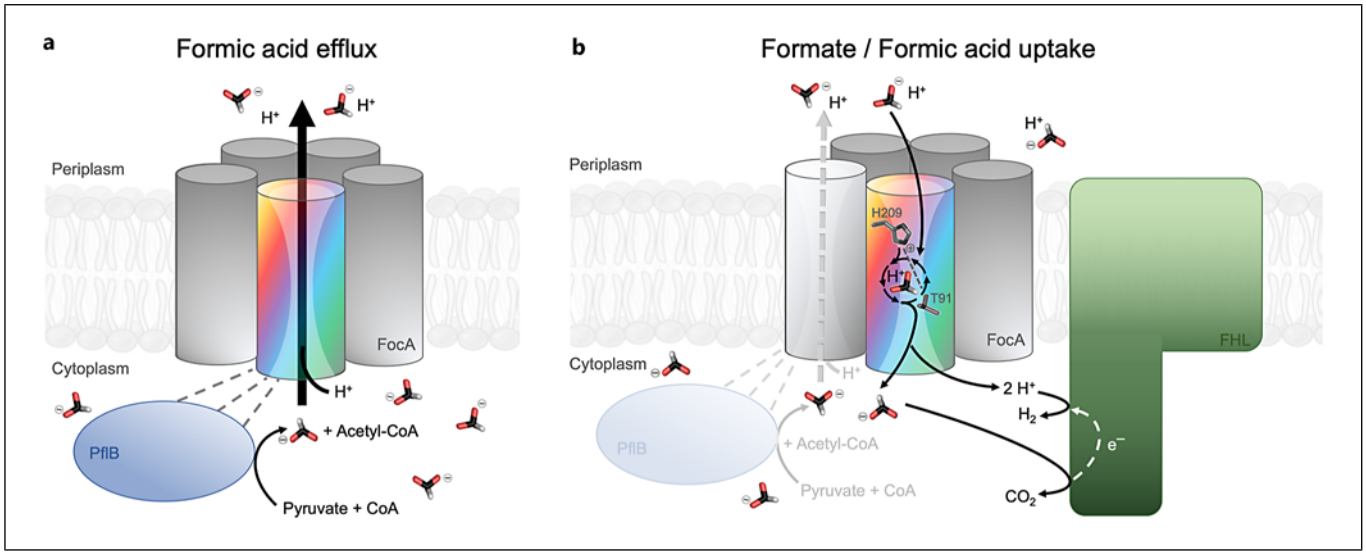

Fig. 1. Schematic representation of the FocA pentamer in the cytoplasmic membrane of *E. coli* and our current understanding of how the bacterium bidirectionally translocates formate or formic acid. FocA is displayed in gray with one of the monomers shown in rainbow coloring and with a silhouette of the translocation pore. Formic acid efflux (**a**) is gated by interaction of FocA with the formate-producing enzyme pyruvate formate-lyase (PflB, blue) and occurs in the early exponential growth phase (pH > 6.8). **b** A model for the uptake of formate or formic acid by FocA. Upon acidification (pH < 6.8) of the periplasmic space, e.g., upon entry into the late-exponential, early stationary phase of growth, formate or formic acid is imported and this is dependent on an active formate hydrogenlyase complex (FHL-1; green). The uptake of the anion, formate, at low concentration, is suggested to involve a transient protonation-recapture mechanism involving the H209 and T91 network, as described [2, 25]. At high external formate concentration, proton-driven formic acid translocation is proposed to occur, whereby the formic acid is directed toward the FHL-1 complex [16].

formate in the stationary phase, which is not observed with cells synthesizing efflux-only variants.

Together, these data suggest that the mechanisms of formic acid efflux and formate or formic acid import differ, a proposal borne out by the fact that the toxic formate analog, hypophosphite, can only be imported by cells synthesizing native FocA with a histidine at residue position 209 [21, 23]. These data strongly suggest that at low pH, H209 (pK_a = 6) is important for a protonation step in the import of formate into the cell (shown in Fig. 1). Moreover, because hypophosphite has a pK_a of 1.1, at physiological pH, it will be present almost exclusively as its dissociated conjugate base. Due to the hydrophobic nature of FocA's pore, only neutral and uncharged molecules like hypophosphorous acid or formic acid (pK_a = 3.75) can be translocated across the narrow core of the pore, requiring a strongly protonating residue to neutralize these strong conjugate bases during translocation [2, 14, 25].

While the role of protonation of H209 at low pH during fermentation appears to be clearly important in uptake of formate or formic acid, it is still unclear to what extent hydrogen-bonding between H209 and T91 plays a role in the bidirectional translocation of formate or formic acid by native FocA and whether it is decisive for one of the two main $FocA_{H209}$ phenotypes (the formic acid efflux-only phenotype, or the intracellular formate accumulation phenotype) observed in *E. coli* cells synthesizing $FocA_{H209}$ variants. In the current study, we replaced H209 with either cysteine or serine, both of which have similar steric properties, but differ in their ability to form hydrogen bonds, and they also differ in their reactivity [2, 26–28]. Cysteine has a solution pK_a of 8.3 and at physiological pH exists mainly as the protonated thiol species; however, the thiol group can be deprotonated to a minor extent, even at pH 7, delivering the negatively charged thiolate anion. While the hydroxyl group of serine more readily forms hydrogen bonds than the thiol, the sulfur atom of cysteine is considerably more reactive, particularly the thiolate species, than the oxygen atom of the hydroxyl group [28]. Surprisingly, the findings of our study indicate that the simple exchange of the oxygen atom in a serine residue for the sulfur of a cysteine residue generates a $FocA_{H209C}$ variant with a unique phenotype, which differs considerably from that of a strain producing a

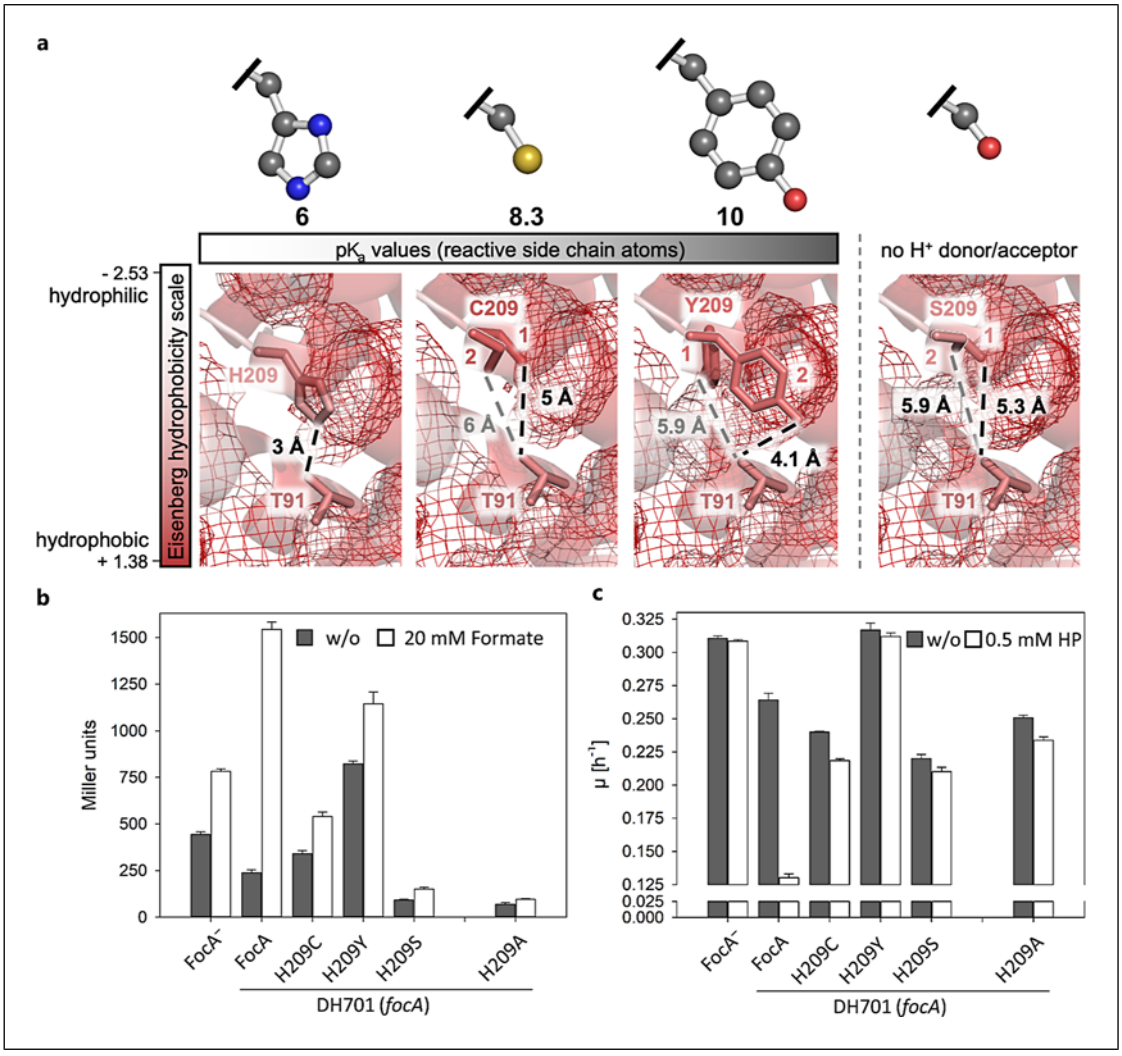

Fig. 2. Analysis of strains synthesizing plasmid-encoded FocA variants with residue exchanges at position 209. **a** A structural representation of the central part of the pore of $FocA_{H209}$ exchange variants (based on the structure of FocA [22]; PDB: 3KLY). Histidine-209 was substituted with cysteine, serine, or tyrosine in silico using the mutagenesis and distance measurement tool of PyMOL. The secondary structures are displayed in the cartoon representation with its surface illustrated as a wire frame and coloring followed the Eisenberg hydrophobicity scale. **b** The effect of exchanges at residue 209 of FocA in strains monitored by measuring β-galactosidase enzyme activity expressed from the formate-responsive *fdhF*$_P$::*lacZ* reporter. Strains were cultivated anaerobically in M9-glucose minimal medium with either no addition (dark gray histograms), or with the addition of 20 mM sodium formate (white histograms). The *focA* mutant DH701(FocA$^-$) was transformed with plasmids carrying the native *focA* gene (FocA), or mutated *focA* genes encoding FocA with an amino acid substitution at residue 209 (indicated by the replaced residue H209X). The β-galactosidase enzyme activity was determined in the early exponential phase (OD_{600} ~ 0.7–0.9) of growth. **c** The sensitivity of the *focA* mutant DH701(FocA$^-$) and DH701 complemented with plasmids encoding FocA and substitution variants (referred to as H209X), toward hypophosphite, which was assessed by analysis of anaerobic growth rates in M9-glucose minimal medium without any addition (dark gray histogram), or in the presence of 0.5 mM sodium hypophosphite (white histogram). The experiments were performed with minimally three biological replicates, each assay carried out in triplicate and data are presented with standard deviation of the mean.

$FocA_{H209S}$ variant. Characterization of an *E. coli* strain synthesizing a $FocA_{H209C}$ variant supports our contention that distinct mechanisms govern bidirectional translocation of formic acid but also strongly suggest that there are two mechanisms involved in the uptake of formate or formic acid. These mechanisms appear to differ in dependence on the concentration of the acid or its anion, formate, and on whether formate originates

from an endogenous or an exogenous source. These data potentially provide an explanation for the highly meaningful findings on formate metabolism presented in a recent publication [16].

Methods

Bacterial Strains and General Growth Conditions

The growth conditions of the strains (shown in online suppl. Table S1; for all online suppl. material, see https://doi.org/10.1159/000548185) applied in this study were exactly as described [29]. Anaerobic cultivation was performed in M9 minimal medium [29, 30] with 0.8% (w/v) glucose as carbon source, and at 37°C. Growth of *E. coli* BL21 (DE3) transformed with derivatives of plasmid pfocA3 for the overproduction and purification of *C*-terminally StrepII-tagged FocA and its variants, was carried out in 400 mL of TB medium (1.2% w/v tryptone, 2.4% w/v yeast extract, 0.4% w/v glycerol, 0.8% w/v glucose, 100 mM potassium phosphate, pH 7) in a baffled 1 L Erlenmeyer flask with shaking, as described [29].

Sodium salts of formate and hypophosphite were added where indicated to a final concentration of 20 mM and 0.5 mM, respectively. When required, antibiotics were used at a final concentration of 100 μg mL^{-1} for kanamycin and 150 μg mL^{-1} for ampicillin.

Construction of Strains and Plasmids

Plasmids encoding the wild-type *E. coli focA* gene (pfocA) [23] and the *focA* gene fused with the DNA sequence encoding a *C*-terminal StrepII-tag (pfocA3) [31] were used in this study (shown in online suppl. Table S1). Plasmids pfocA and pfocA3 served as templates for site-directed mutagenesis of codon 209 (for histidine), which was exchanged for codons decoding as the amino acids A, C, S or Y, using the oligonucleotide primers listed in online supplementary Table S2. Oligonucleotides were obtained from IDT BVBA (Interleuvenlaan, Belgium) and mutagenesis was performed as previously reported [23]. All introduced site-specific mutations were verified by DNA sequence analysis of the complete *focA* gene.

The chromosomal substitution of *focA* codon 209 to a cysteine codon (TGC) was carried out using an established protocol [23]. The template for site-directed mutagenesis was pMAK705::*focA*-H209N [23] and the oligonucleotides focA_H209C_fw and focA_H209C_rev were used to replace codon 209 (shown in online supppl. Table S2). The *focA* allele of pMAK705::*focA* H209C was recombined into the chromosome of strain MC4100 [32], yielding strain MC4400.

The *fhlA* mutant, DH5000, was generated using $P1_{kc}$-mediated transduction with the phage grown on strain JW2701 (the KEIO collection *fhlA* deletion strain [33]) following the procedure of Miller [34], which introduced a kanamycin-resistance cassette in place of the *fhlA* gene. Subsequent removal of this cassette within the mutated gene was done following the method of Cherepanov and Wackernagel using the temperature-sensitive plasmid pCP20 [35]. This procedure resulted in the strain MC5000 and the presence of the *fhlA* deletion mutation was verified by colony PCR. The corresponding formate-reporter strains of MC4400 and MC5000 were created by transfection with phage λ (*$fdhF_P$::lacZ*) [15] (shown in online suppl. Table S1), yielding DH4400 and DH5000, respectively.

Overproduction and Purification of StrepII-Tagged FocA and Its Amino Acid-Exchange Variants

In order to overproduce native FocA and selected amino acid-exchange variants carrying a *C*-terminal StrepII-tag, the cultivation was performed exactly as previously described [29]. Cell harvest, disruption, membrane solubilization, and purification applying Strep-Tactin-based affinity chromatography followed the described protocol [29]. The procedure yielded 0.1–0.2 mg of purified FocA protein l^{-1} of culture.

Polyacrylamide Gel Electrophoresis and Immunoblotting

The purified FocA proteins were either separated by denaturing SDS-polyacrylamide gel electrophoresis (PAGE) using 12.5% (w/v) polyacrylamide gels [36], or by blue-native PAGE using precast 4–16% gradient gels from SERVA Electrophoresis GmbH (Heidelberg, Germany) [37] as described [31]. Subsequent silver staining to visualize polypeptides was carried out according to the method described in the Pierce Silver-staining kit (Thermo Fisher Scientific, Dreieich, Germany). Immunodetection analysis was done using anti-FocA antiserum (diluted 1:1,000), which included antibodies raised in rabbits against full-length, native FocA (Methods, see [29].

Circular Dichroism Spectroscopy

Before far-UV spectra were recorded, a buffer-exchange was done by dialysis against 100 mM Tris/HCl buffer, pH 8, including 150 mM NaCl, 2 mM dodecyl maltoside using Spectra/Por® cellulose membrane tubes with a molecular mass cutoff of 10 kDa. The dialysis

buffer was exchanged twice. Approximately 100 µL of the purified protein samples (~30–40 µg) were transferred into a 0.05-cm cuvette (Quartz Glass Suprasil from Hellma Analytics, Muellheim, Germany). The measurement of the ellipticity in the wavelength range of 190–250 nm was carried out on a Jasco J710 spectropolarimeter at 20°C with a speed of 1 nm s^{-1} with 64 accumulations, similar to the protocol described [31]. The data were corrected for the buffer signal and the molar ellipticity [Θ] was calculated with the following formula: $[\Theta] = \frac{\Theta \times M}{1000 \times n_A \times c \times I}$ (Θ, measured signal; M, molecular weight of the protein in Da; n_A, number of amino acids in the protein; c, protein concentration in g mL^{-1}; I, thickness of cuvette in cm).

Hypophosphite-Sensitivity Test and Analysis of Intra- and Extracellular Formate Levels

Growth of selected *E. coli* strains was performed anaerobically in M9 minimal medium containing 0.8% (w/v) glucose at 37°C. The determination of anaerobic growth rates and the effect of 0.5 mM sodium hypophosphite on the growth rate was carried out in microtiter plates as previously described [29]. The analysis of changes in intracellular formate levels via the β-galactosidase enzyme activity assay was done exactly as described [23, 29]. Determination of formate and lactate concentrations in the growth medium was done by high-performance liquid chromatography [23]. Unless otherwise noted, the samples for the determination of β-galactosidase enzyme activity and for extracellular formate concentration were taken when cells reached the late exponential phase ($OD_{600\ nm}$ ~ 0.7–0.85) of growth. The experiments were performed minimally in duplicate with minimally three biological replicates and data are presented as standard deviation of the mean.

Analysis of H_2 Production via Gas Chromatography

Accumulated H_2 was measured in the headspace of cultures grown anaerobically for 24 h in 15 mL Hungate tubes in M9-glucose minimal medium (10 mL headspace), initially under a N_2 atmosphere, and at 37°C [23]. The experiments were done twice, each with three biological replicates, and the amount of H_2 was calculated with reference to the optical density ($OD_{600\ nm}$) and is presented as standard deviation of the mean.

Computational Analysis

The crystal structure of the *V. cholerae* FocA protein (PDB: 3KLY) was used to depict the central hydrophobic part of the translocation pore of FocA [22] but using the amino acid numbering based on the *E. coli* FocA protein. The in silico mutagenesis tool of PyMOL (The PyMOL Molecular Graphics System, version 2.5, Schrödinger, LLC) was used to generate figures for visualization of the side-chain orientation in *E. coli* $FocA_{H209}$ variants. These structures are shown in cartoon representation with grids, and the protein backbones and the chosen side chains are colored according to the Eisenberg hydrophobicity scale [38]. Determination of the distances between residue 209's side chain and that of the threonine residue, T91 was also carried out using PyMOL.

Results

A $FocA_{H209C}$ Variant Shows Near-Wild-Type Formic Acid Efflux but Impaired Formate Uptake in vivo

Findings from previously reported in vivo mutational analyses [21, 23] are consistent with the conserved H209 residue in FocA protonating formate during its translocation through the hydrophobic core of FocA's pore, in particular in the import direction. In order to determine what impact an amino acid residue with a thiol or hydroxyl side chain might have on bidirectional formate or formic acid translocation, three new amino acid variants of FocA with a cysteine, a serine or a tyrosine in place of H209 were constructed. With a pK_a of 8.3, cysteine represents an amino acid residue whose thiol group is only poorly deprotonated at physiological pH [28] (shown in Fig. 2a), while substitution of the thiol with the hydroxyl group of serine introduces a residue that typically cannot be readily deprotonated [39]. While both thiol and hydroxyl groups are capable of hydrogen-bonding with T91, the predicted distance between either residue and T91 would be more than 5 Å, which is too great for a hydrogen bond (typically 2.5–3.2 Å) to form (shown in Fig. 2a). The H209Y variant of FocA was constructed as a control to determine the consequence of introducing a bulky aryl hydroxyl group, which, with a pK_a = 10 is not readily deprotonated at physiological pH, and its separation from T91 also indicates that no hydrogen bond should form (shown in Fig. 2a). Plasmids carrying the genes encoding these FocA variants (shown in online suppl. Table S1) were introduced into the *focA* mutant strain, DH701, which carries a genomic copy of the formate-responsive reporter, *$fdhF_P$::lacZ* [15]. After anaerobic growth of the strains to the late exponential phase in M9-glucose minimal medium, changes in, or differences between, intracellular formate levels of the strains were monitored by determining β-galactosidase enzyme activity (shown in Fig. 2b).

The *focA* mutant, DH701, had a β-galactosidase enzyme activity that was approximately 450 U. This level of

activity was reduced by nearly half when the native *focA* gene was reintroduced into the strain on plasmid pfocA (encoding FocA without a StrepII-tag, online suppl. Table S1), which indicates that less formate was present intracellularly and a minor enhancement of formic acid efflux had occurred (shown in online suppl. Fig. S1). Introduction of plasmid pfocA-H209C, encoding $FocA_{H209C}$, into DH701 resulted in a β-galactosidase enzyme activity that was between that of the strain DH701 and DH701 transformed with pfocA (75% of enzyme activity compared to DH701; shown in Fig. 2b). This result indicates that the $FocA_{H209C}$ variant was functional in formic acid efflux, but was less efficient at translocating the organic acid across the membrane compared with native FocA. This was an unexpected and new phenotype for a strain synthesizing a FocA variant with a residue exchange of H209.

Exchange of H209 in FocA for a serine residue resulted in a phenotype characteristic of enhanced efflux of formic acid, whereby a lower intracellular level of formate (92 ± 5 U), compared with even that of the *focA* mutant DH701, was determined (shown in Fig. 2b), and, significantly, extracellular formate was increased, with about 2.3-fold more formate than was measured for the strain DH701 transformed with pfocA (shown in online suppl. Fig. S1). These phenotypes of strongly reduced intracellular formate levels and increased formic acid efflux were similar to those observed for strain DH701 synthesizing a FocA variant with an alanine residue substituted for H209 (shown in Fig. 2b; online suppl. Fig. S1), and which was reported previously for efflux-only $FocA_{H209}$ variants [21].

In contrast, strain DH701 synthesizing $FocA_{H209Y}$ resulted in a β-galactosidase enzyme activity of approximately 820 U, indicating intracellular accumulation of formate, presumably due to impaired efflux of formic acid by the bulkier tyrosine residue of $FocA_{H209Y}$ (shown in Fig. 2a). This was also reflected in decreased extracellular formate levels measured in the growth medium for the strain (shown in online suppl. Fig. S1). This phenotype for in vivo formate translocation, in which the strain accumulated formate intracellularly, was similar to that observed previously when the same strain synthesized FocA variants with bulky residues at this residue position and which were predicted to impede translocation of formic acid through the pore [21]. Together, these findings indicate that, while serine and tyrosine exchanges at residue position 209 delivered either of the two known and previously characterized translocation phenotypes, the cysteine-exchange variant delivered a new intermediary phenotype in which formic acid efflux was more similar to, but nevertheless less effective than, that of the native FocA. This suggests that the exchange of a sulfur for an oxygen atom (compare $FocA_{H209C}$ with $FocA_{H209S}$) is sufficient to result in retention of at least partial control of formic acid efflux activity, similar to that observed when a histidine is present at this position.

To determine whether exogenously supplied formate could be imported by DH701 synthesizing these amino acid-exchange variants of FocA, the experiment was also repeated with 20 mM sodium formate added to the growth medium (shown in Fig. 2b). While formate addition only mildly increased expression of the *fdhF*$_P$::*lacZ* fusion in strain DH701 (*focA*) lacking FocA, the exogenous formate addition caused an approximate 6.5-fold increase in the β-galactosidase enzyme activity (*ca.* 1540 U) measured for strain DH701 carrying plasmid pfocA, encoding native FocA (shown in Fig. 2b). This result indicates that efficient formate or formic acid transport into the cell occurred, with a consequent increase in *lacZ* reporter expression, as anticipated [7, 13, 15]. In contrast, addition of formate to strain DH701/pfocA-H209C caused only a minor increase in *lacZ* expression (shown in Fig. 2b), strongly suggesting that this $FocA_{H209C}$ variant was severely impaired in formate or formic acid uptake. When strain DH701 synthesized the $FocA_{H209S}$ variant, addition of exogenous formate to the growth medium had little impact on β-galactosidase enzyme activity, which is similar to what was observed when the $FocA_{H209A}$ variant was synthesized in the strain (shown in Fig. 2b). This efflux-only phenotype is also characteristic for a strain synthesizing the $FocA_{H209N}$ variant [23].

When strain DH701 was transformed with plasmid pfocA-H209Y, supplementation of formate to the growth medium caused an approximately 40% increase in β-galactosidase enzyme activity (shown in Fig. 2b), which is similar to what was previously observed when the strain synthesized $FocA_{H209F}$ or $FocA_{H209W}$ [21].

Finally, we examined the effect of the toxic formate analog, sodium hypophosphite [13], on anaerobic growth of the strains (shown in Fig. 2c). When supplied at a concentration of 0.5 mM to the M9-glucose growth medium, the anaerobic growth rate of strain DH701/pfocA was reduced by approximately 50%, while the growth rate of the *focA* mutant strain (DH701) was unaffected by the presence of hypophosphite. This result demonstrates that under these conditions hypophosphite uptake is dependent on FocA, as has been shown previously [13, 23], and provides an alternative means of examining the effect of the amino acid exchanges on the functionality of the FocA variants in the import direction. Strain DH701 synthesizing either $FocA_{H209Y}$, $FocA_{H209S}$, or $FocA_{H209A}$ showed hardly any negative impact of hypophosphite on the anaerobic growth rate, and strain DH701 synthesizing $FocA_{H209C}$ also showed only a very weak reduction in its

anaerobic growth rate of approximately 9% compared to the anaerobic growth rate in the absence of hypophosphite (shown in Fig. 2c). These results further underline that exchange of H209 for any other amino acid severely impairs uptake of the formate analog, hypophosphite. It is nevertheless notable that, without hypophosphite addition, the strain synthesizing $FocA_{H209C}$ showed a reduced growth rate similar to that for the strain synthesizing $FocA_{H209S}$ and $FocA_{H209A}$ (shown in Fig. 2c). This may be linked to the reduced apparent efficiency of formic acid efflux by the strain.

The $FocA_{H209C}$ variant has similar secondary and quaternary structural characteristics compared to the native protein. The pentameric FocA protein has six major transmembrane helices and forms a generally stable structure in the cytoplasmic membrane [13, 17] (shown in Fig. 3a, b). To determine whether the residue exchange in $FocA_{H209C}$ had any impact on the structure and stability of the protein in the *E. coli* cell, a *C*-terminally StrepII-tagged version of the protein was isolated and compared in several of its biophysical properties with the native FocA protein and with the purified $FocA_{H209A}$ variant. With the exception of the reduced protein yield of $FocA_{H209A}$ and $FocA_{H209C}$ compared to the native FocA, all three proteins could be stably overproduced and purified (shown in Fig. 3c) and were confirmed to be FocA in Western blot analysis with anti-FocA-specific antiserum (shown in Fig. 3d).

FocA is a pentamer in the cytoplasmic membrane (shown in Fig. 3a) but frequently migrates as a dimer of pentamers in blue-native PAGE [40]. All three purified FocA proteins analyzed in this current study migrated as dimers of pentamers with an apparent molecular mass of approximately 350 kDa (shown in Fig. 3e) (monomeric mass of 31 kDa without StrepII-tag). Finally, the secondary structural features of StepII-tagged native FocA and $FocA_{H209C}$ were analyzed by circular dichroism (CD) and shown to have near-identical secondary structural content, exhibiting the typical CD curve for an α-helical protein, such as for FocA [31] (shown in Fig. 3f). Taken together, these data indicate that the $FocA_{H209C}$ variant and native FocA have indistinguishable biophysical characteristics in vitro.

Genomic Integration of the Mutated focA *Gene Confirms Inability of $FocA_{H209C}$ to Facilitate Import of Formate or Hypophosphite*

Chromosomal integration of the mutated *focA* gene encoding $FocA_{H209C}$ delivered strain DH4400 (see Methods; online suppl. Table S1). Analysis of formate levels in the culture medium after anaerobic growth in M9-glucose minimal medium revealed a steady accumulation of formate throughout the growth phase. The highest levels of formate, 8.9 ± 1.1 mM OD_{600}^{-1}, were measured in the late stationary phase of growth for DH4400 (shown in Fig. 4a). This contrasts the situation with strain DH4100, encoding native FocA, which showed a slight reduction in extracellular levels of formate in late stationary phase cultures of ca. 7 mM OD_{600}^{-1}. Otherwise, the amount of formate excreted by both strains was similar, especially in exponential-phase cultures (shown in Fig. 4a). Analysis of the *focA* mutant strain, DH701, revealed that late stationary phase cells of the strain excreted less formate (4.3 ± 0.3 mM OD_{600}^{-1}) compared with either the parental strain DH4100 or strain DH4400 synthesizing $FocA_{H209C}$ (shown in Fig. 4a).

Two strains known not to reimport formate include DH4200 [23] and a strain unable to synthesize an active FHL-1 complex [15]. For example, a *fhlA* mutant lacks the formate-responsive transcriptional regulator FhlA, which controls expression of the formate regulon [7], and therefore fails to synthesize FHL-1 [8, 41]. Therefore, as a control to examine formate translocation in strains known to be restricted in the import of formate, an isogenic *fhlA* mutant, DH5000 (online suppl. Table S1), was constructed and formate excretion into the culture medium was determined for strains DH4200 (synthesizes $FocA_{H209N}$) and DH5000 (no FhlA) during anaerobic growth in M9-glucose minimal medium (shown in Fig. 4a). The results clearly showed for both strains a steady accumulation of formate in the culture medium and, for both strains, formate accumulated to higher concentrations than for the parental strain, DH4100. Moreover, the level of formate in the medium of late stationary phase cultures was considerably higher than in other phases of cultivation, suggesting that these strains, along with DH4400, failed to reimport formate efficiently.

Analysis of changes in intracellular formate levels throughout the growth phase in all five strains revealed increased levels of β-galactosidase enzyme activity over time, reflecting high intracellular formate levels, for the parental strain DH4100, the *focA* mutant DH701 and strain DH4400, encoding $FocA_{H209C}$, in both exponential and early stationary phases (shown in Fig. 4b). Higher enzyme activity levels for strains DH701 and DH4400 indicate higher intracellular formate accumulation compared with the parental strain DH4100 [13, 15]. This demonstrates that the lack of FocA (DH701), or synthesis of $FocA_{H209C}$ (DH4400) with marginally impaired efflux function, results in accumulation of the anion inside the cell. Intracellular levels of formate were, however, strongly reduced in late stationary phase cultures (9-fold for

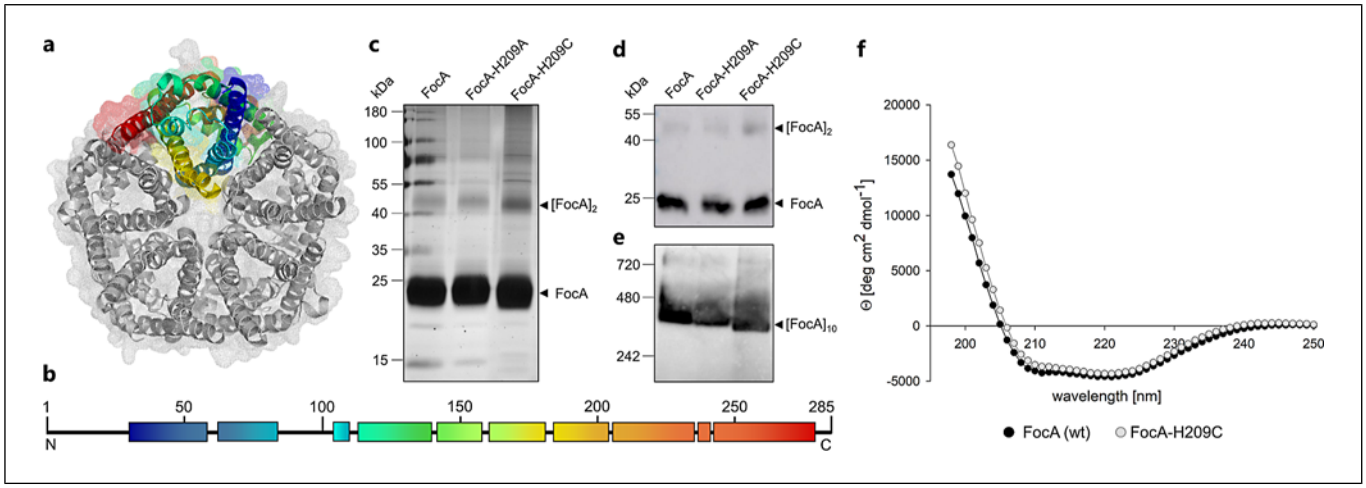

Fig. 3. $FocA_{H209}$ variants are synthesized as predominantly α-helical membrane-integral proteins. **a** A structural overview of the *V. cholerae* FocA pentamer (PDB: 3KLY) but using residue-numbering for *E. coli* FocA. One of the monomers is highlighted with rainbow coloring from the proteins' *N*-terminus (blue) to the *C*-terminus (red). The secondary structures are displayed in the cartoon representation with its surface illustrated as a "wire frame". **b** A schematic representation of secondary structural elements of FocA from *V. cholerae* based on X-ray data of [22]. The α-helical elements from residues 29 to 280 are depicted as boxes following the color-coding of **a**. Unstructured regions and loops are displayed as a horizontal line. **c** Native *E. coli* FocA and the $FocA_{H209C}$ variant, both carrying a *C*-terminal Strep(II)-tag, analyzed after affinity chromatographic purification. Aliquots of 5 µg protein were separated in a 12.5% (w/v) SDS-PAGE and subsequently the gel was silver-stained. The migration positions of the molecular mass marker (PageRuler Prestained Protein Ladder, Thermo Fisher Scientific) are shown in kDa on the left side and the arrows indicate the FocA monomeric [FocA] or the dimeric, incompletely denatured, form of the protein $[FocA]_2$. Western immunoblots of purified FocA samples (2 µg protein) that were separated under denaturing conditions (12.5% SDS gel, **d**) and under non-denaturing conditions in a native gradient gel (4–16% acrylamide SERVA, **e**). After the transfer to a nitrocellulose membrane, FocA was detected with antibodies raised against the full-length FocA protein (antiserum was diluted 1:1,000, see Experimental procedures). Molecular mass markers PageRuler Prestained Protein Ladder (**d**), a Native Marker Liquid Mix from SERVA (**e**) were used, and the corresponding molecular mass is depicted in kDa on the left side of the gels. Arrows indicate the FocA monomer [FocA], a dimer $[FocA]_2$ or a decamer $[FocA]_{10}$. **f** A far-UV CD-spectroscopic analysis of *C*-terminally StrepII-tagged FocA (black) and $FocA_{H209C}$ (gray). The purified proteins had a concentration of 0.41 mg mL^{-1} (FocA) and 0.29 mg mL^{-1} ($FocA_{H209C}$) and the spectra were adjusted to account for the concentration difference. The ellipticity was recorded in the wavelength range of 190–250 nm at 20°C using 0.05-cm quartz cuvettes. In total, 64 accumulations were measured and datasets were corrected with the buffer signal.

DH4100, 15-fold for DH701, and 4-fold for DH4400) compared to the early stationary phase, indicating either enhanced formate efflux by the strains or disproportionation of formic acid by the FHL-1 complex, causing reduction in FhlA-dependent *fdhF*$_P$::*lacZ* expression (shown in Fig. 4b). Strain DH4400 nevertheless had roughly 4-fold higher levels of intracellular formate compared with the parental strain, DH4100.

Strain DH4200 synthesizing $FocA_{H209N}$ showed approximately 3- to 4-fold lower levels of intracellular formate in the exponential and early stationary growth phases compared with the level present in DH4100 (shown in Fig. 4b). In contrast, strain DH5000 (Δ*fhlA*) failed to generate β-galactosidase enzyme activity because it lacks the formate-responsive transcriptional regulator, FhlA, and therefore cannot induce *fdhF*$_P$::*lacZ* expression [41].

Measurement of accumulated H_2 by the formate-inducible FHL-1 complex in stationary phase cultures revealed that strains DH4100, DH701, and DH4400 all produced H_2 in the range of 90–110 µmol H_2 OD_{600}^{-1} (shown in Fig. S2). In contrast, strain DH5000 (Δ*fhlA*) failed to produce any H_2, as anticipated [7, 41], while strain DH4200 accumulated barely detectable levels of the gas (shown in online suppl. Fig. S2). The levels of H_2 produced by the different strains correlated with the intracellular levels of β-galactosidase enzyme activity measured for those respective strains, and cultures of strain DH4400 produced only approximately 5% more H_2 than cultures of the parental strain DH4100 (compare Fig. 4b, and online suppl. Fig. S2). These data suggest that the reduction in intracellular formate measured in stationary-phase cells of DH4400 resulted only partially

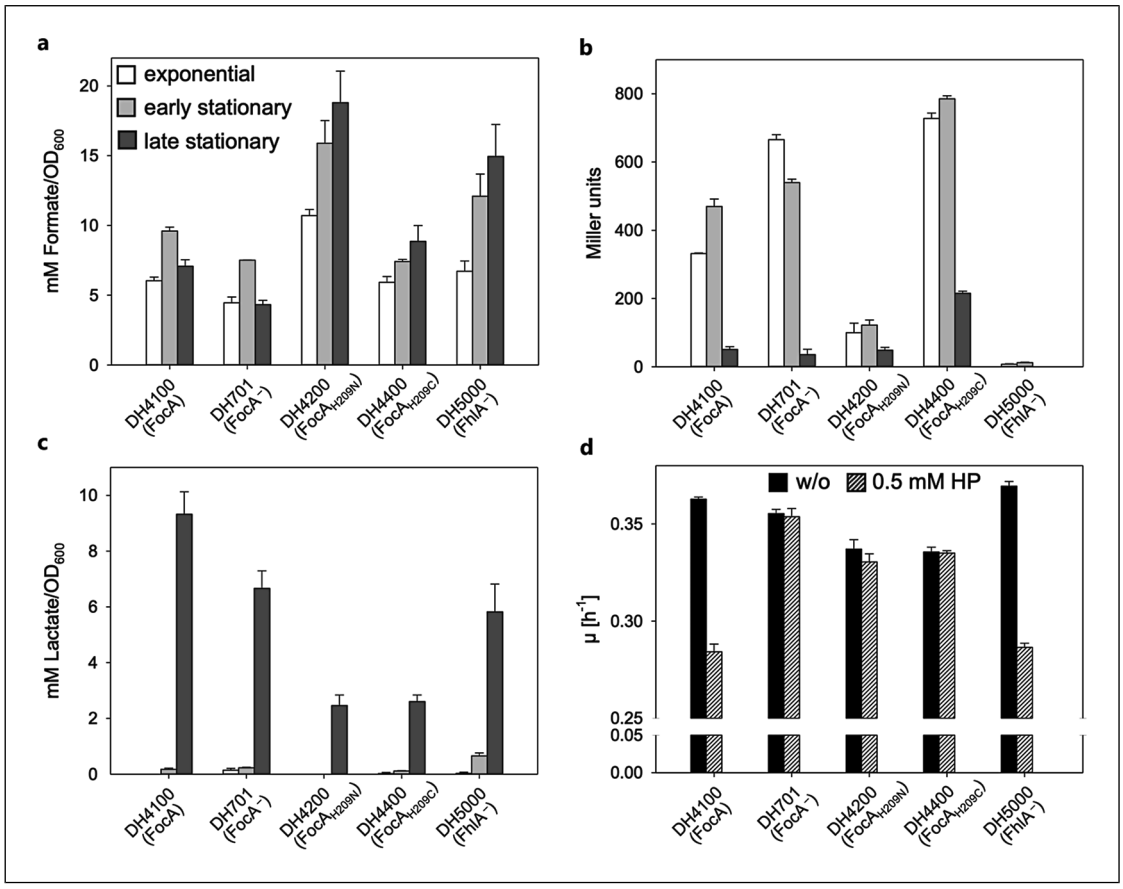

Fig. 4. Controlled bidirectional formate/formic acid translocation depends on FocA's T91-H209 axis and an active FHL-1 complex. **a** The formate concentration measured in culture supernatants of exponential phase (OD_{600} = 0.64–0.82; after approximately 4–6 h' growth), early (OD_{600} = 0.92–1.41; after approximately 6–7 h' growth), and late stationary phase (OD_{600} = 0.87–1.59; after 24 h of cultivation) of the parental strain DH4100 (FocA), the *focA* mutant DH701(FocA$^-$), strain DH4200 ($FocA_{H209N}$), strain DH4400 ($FocA_{H209C}$), and strain DH5000 (Δ*fhlA*). **b**, **c** The β-galactosidase enzyme activity and the lactate concentration in the same cultures and growth phases, respectively, as in **a**. **d** Sensitivity of the strains toward hypophosphite was assessed by analysis of anaerobic growth rates in M9-glucose minimal medium without (w/o) and in the presence of 0.5 mM sodium hypophosphite. The experiments were performed with minimally three biological replicates, each assay was carried out in duplicate, and data are represented with standard deviation of the mean.

from its disproportion and partially from efflux by FocA$_{H209C}$. However, the fact that the *focA* mutant DH701 showed similar profiles for both *fdhF$_P$*::*lacZ* expression and only a small decrease in H_2 production indicates that the conclusion that DH4400 is capable of formic acid efflux must be interpreted with care at this stage.

Determination of Lactate Excretion in Late Stationary Phase Cultures Reveals Parallels between Strains Synthesizing FocA$_{H209N}$ and FocA$_{H209C}$

Lactate is excreted as a fermentation product to help in balancing the redox state of the pyridine nucleotide pools and in the maintenance of pH homeostasis [1]. Virtually no lactate was detectable in exponential or early stationary phase cultures for four of the five strains analyzed (shown in Fig. 4c). The exception was for strain DH5000 (Δ*fhlA*) in early stationary phase cultures where 0.6 ± 0.1 mM lactate per OD_{600} was determined. In late stationary phase cultures considerably higher levels of lactate were measured. The highest concentration was produced by the parental strain DH4100, which generated just over 9 mM lactate per unit OD_{600} (shown in Fig. 4c). This was followed by strains DH701 (*focA*) and DH5000 (Δ*fhlA*), which both produced approximately 7 mM lactate per OD_{600} (shown in Fig. 4c). Strains DH4200 (synthesizes $FocA_{H209N}$) and DH4400 (synthesizes $FocA_{H209C}$) both produced between 2 mM and 3 mM lactate per OD_{600}, which was approximately a 4-

fold lower amount compared with the parental strain DH4100. These data suggest that both of these strains share a common phenotype with respect to their fermentation product spectrum.

A strain lacking a functional FHL complex remains sensitive to the toxic formate analog, hypophosphite. The uptake of hypophosphite has been shown to be FocA-dependent and results in a reduced anaerobic growth rate [13, 29]. Under the conditions used in this experiment, the growth rate of the parental strain, DH4100, was reduced by more than 20% when cells were grown in the presence of 0.5 mM sodium hypophosphite (shown in Fig. 4d). In contrast, neither of the strains DH701 (*focA*), DH4200 (synthesizes $FocA_{H209N}$) nor DH4400 (synthesizes $FocA_{H209C}$) showed a reduced growth rate when cultivated anaerobically in the presence of hypophosphite. However, the *fhlA* mutant, DH5000, despite being unable to synthesize a functional FHL-1 complex, showed a similar level of sensitivity to hypophosphite compared with the parental strain, DH4100 (shown in Fig. 4d). This finding indicates that, while mutants unable to synthesize an active FHL-1 complex fail to take up exogenously supplied formate [15], uptake of hypophosphite nevertheless occurs and is thus independent of an active FHL-1 complex.

Discussion

A cysteine-for-histidine substitution of the highly conserved residue H209 within the pore of FocA delivered a protein variant that presents a so-far unique phenotype with respect to formate/formic acid translocation across the cytoplasmic membrane. In the efflux direction, cells synthesizing the chromosomally encoded $FocA_{H209C}$ variant translocate formic acid out of the cell with poorer efficiency than cells synthesizing the native FocA protein; more importantly, however, in the uptake direction, a strain synthesizing $FocA_{H209C}$ appears to fail to import formate effectively (shown in Fig. 4). The other two main phenotypes observed in strains synthesizing FocA variants with amino acid exchanges at H209 either show enhanced formic acid efflux, e.g., in N209, A209, I209, T209, and as shown in this study, S209 variants, with essentially no formate uptake, or they exhibit impaired formic acid efflux, e.g., in D209, E209, W209, F209, or Y209 variants, but these variants all allow limited formate uptake in stationary-phase cells when it is added exogenously [21, 23]. Importantly, however, no amino acid variant in which H209 is exchanged for any other amino acid residue is capable of importing hypophosphite, including strain DH4400, which synthesizes $FocA_{H209C}$. As histidine is the only amino acid residue that can serve as a proton acceptor or donor under physiological pH conditions and because hypophosphite with a pK_a of 1.1 is essentially always present as the anionic, deprotonated species, this strongly suggests that protonation of hypophosphite, and by analogy formate (pK_a of 3.75), is important during the import of these anions [2, 14]. Protonation of these species is proposed to be essential to allow transit of these acids through the hydrophobic pore of FocA [25]. Thus, the question arises: how do strains synthesizing certain FocA variants (e.g., D209 or Y209) allow import of some formate but do not translocate hypophosphite?

The formate-translocation phenotypes of the different FocA variants described recently [21, 23] and in this study are consistent with FocA employing two mechanisms to translocate formate/formic acid into the cell. In their recent paper, Metcalfe et al. [16], by using elegantly designed labeling experiments combined with a variety of sophisticated spectroscopic detection methods, demonstrated very clearly that *E. coli* cells growing anaerobically on glucose can distinguish between formate that has been generated intracellularly, i.e., where it is generated internally by the PflB reaction then translocated across the membrane and is then reimported, from sodium formate that has been supplied exogenously to the culture and is imported into the cell. While the authors worked exclusively with a wild-type strain in that study [16], the findings presented in this current study are entirely consistent with FocA being responsible for both types of formate uptake observed by Metcalfe et al. [16]. In particular, when high concentrations of exogenous formate are added to the cultures, uptake appears to be proton-coupled, with formic acid being quantitatively directed to the FHL-1 complex, where it is all disproportionated to H_2 and CO_2. This uptake mechanism does not appear to be completely dependent on the histidine residue at amino acid position 209 in FocA and may also account for the partial translocation ability of strains synthesizing some of the FocA variants described above, including $FocA_{Y209}$, which is capable, albeit poorly, of importing some formate. Nevertheless, a portion of this uptake of formic acid may be accountable to free diffusion of formic acid across the membrane, or possibly to a still unidentified further transporter, as was observed for the *focA* mutant, DH701. When FHL-1 is synthesized at maximal levels, e.g., in DH701, due to intracellular formate accumulation during exponential-phase growth, then any formic acid entering the cell by passive diffusion, due to the lower external pH, especially in stationary-phase cultures, will be disproportionated.

The complete dependence on H209 in FocA for import of hypophosphite exemplifies the other uptake mechanism, which clearly relies on highly effective protonation of the anion to allow its passage in neutral form through the central hydrophobic barrier of the pore [17, 18]. This appears to require the conserved histidine-209 residue, as has been proposed recently [2, 25]. Despite changes to the pK_a of amino acid side chains within the microenvironments of a protein being notoriously difficult to predict, it has nevertheless been proposed that the pK_a of histidine decreases in a hydrophobic environment [42]. Such a decrease in the pK_a of H209 would make it a stronger proton donor, thus enhancing the transit of protonated hypophosphite, and consequently also formate, across the hydrophobic barrier and into the cytoplasm. The proposed recapture of the proton by the coupled action of T91 and the imidazolate anion, as has been hypothesized [2, 20, 25], would mean that the anion, and not the acid, would be released into the cytoplasm. This second mechanism is suggested to be how formate at low concentration is reimported into the cytoplasm after being initially translocated out of the cell during fermentation, and when the external pH of the periplasm decreases below 6.5 upon entry of the cells into stationary phase [13, 16]. Notably, cells synthesizing the $FocA_{H209C}$ variant appear to lack the ability to import formate by either mechanism. The reason for this currently remains elusive, but clearly this observed effect is likely conferred by the sulfur atom and will be discussed further below.

In the efflux direction a strain synthesizing $FocA_{H209S}$ very efficiently translocated formic acid out of the cells. This phenotype is characteristic for all variants in which the histidine residue is replaced by any residue with a side chain that is small and uncharged, regardless of whether it can undergo hydrogen-bond formation, or not [21]. Examination of the structure of FocA where the Ω-loop is in the "up" position, placing T91 in the vicinity of H209, strongly suggests that, while H209 is close enough to T91 to form a hydrogen bond, serine or asparagine at this position is not (shown in Fig. 2a). This suggests that if a hydrogen bond cannot be formed, then efflux becomes "uninhibited" and highly efficient, as long as a compact residue with a neutral side chain is introduced. This also agrees with the phenotypes of strains synthesizing FocA variants that have alanine or isoleucine at position 209, as the side chains of these residues cannot form hydrogen bonds. The introduction of bulkier residues at this position, such as tyrosine, phenylalanine or tryptophan, or the charged residues lysine or aspartate block formate efflux, either sterically or electrostatically, respectively. However, this raises the question as to why T91 is essential for not only import but also efflux of formic acid [21, 24]. This might suggest that it is somehow involved in delivering the proton that accompanies formate during efflux [43]. How this might be achieved mechanistically will require further study.

The surprising finding of this study is that a strain synthesizing the cysteine-209 variant of FocA has a very different efflux phenotype compared with a strain synthesizing a variant with a serine residue at this position, despite these near-isosteric residues both having a similar orientation and apparent inability to hydrogen bond with T91 due to distance constraints (shown in virtual mutagenesis studies in Fig. 2a). These data suggest that the presence of the sulfur atom in the $FocA_{H209C}$ variant instead of the oxygen in $FocA_{H209S}$ is responsible for the reduction in formate efflux from the cell. While the efficiency of formic acid efflux by the $FocA_{H209C}$ variant is not restored to that of native FocA, as some formate accumulates inside the cell, formic acid is nonetheless released by the strain (shown in Fig. 4). However, as stated above, the cells synthesizing $FocA_{H209C}$ fail to take up formate, which is also confirmed by the hypophosphite-resistance phenotype exhibited by strain DH4400.

When compared with serine's hydroxyl group, the thiol of cysteine residues within proteins shows the considerably stronger nucleophilicity due to the lone pair of electrons on the sulfur [28]. Moreover, the deprotonated thiolate anion is even more reactive. It is conceivable therefore that the microenvironment around C209 has an impact on the ability of the side chain to react with formic acid, possibly resulting in thioester formation, in analogy with carbon-phosphorus bond formation between cysteine and hypophosphite in PflB [44]. This may obstruct formic acid import through FocA's pore and potentially account for the lower rate of formic acid efflux by the $FocA_{H209C}$ variant. A local pH closer to neutrality will increase the thiolate:thiol ratio of the residue, which also might impede passage of formic acid through the pore. However, at this stage, and with the currently available data, it is difficult to conceive what this reactivity might be and what the consequences for formate or formic acid translocation are. Catalytic cysteine residues in metal-free enzymes are known, for example, in cysteine proteases or protein-tyrosine phosphatases [45], but a lack of other key residues near C209, which would be necessary for such activity, would make this prospect unlikely. Nevertheless, the presence of active-site cysteine residues in certain metal-free formate dehydrogenases makes some form of reactivity for this residue toward formic acid a possibility. Ultimately, structural elucidation of the $FocA_{H209C}$ variant will probably be required to give

further insight into the cause of this unusual in vivo phenotype. Nevertheless, these data further emphasize that the mechanisms underlying the ability of FocA to translocate formate or formic acid bidirectionally is considerably more sophisticated and complex than the simple "opening and closing" of the central pore. This complex translocation appears to allow precise control of formate/formic acid passage, depending on the metabolic status.

Finally, the analysis of the Δ*fhlA* mutant, DH5000, which served as a negative control for key experiments, demonstrated that uptake of hypophosphite, while dependent on FocA, is independent of an active FHL-1 complex. This contrasts with what is observed for formate uptake, which is dependent on an active FHL-1 complex [15]. Expression of the *focA-pflB* operon is independent of the presence of the FhlA transcription factor [7, 46]; therefore, a mutant lacking the regulator still synthesizes FocA, as well as PflB. However, while formate accumulates outside the cell, and not intracellularly, in stationary-phase cells of DH5000, addition of hypophosphite to the culture medium results in a growth-sensitive phenotype. This result indicates that while formate uptake by FocA is coupled with FHL-1 activity, hypophosphite uptake is not. The potential coupling between FocA and the FHL-1 complex in maintaining pH homeostasis supports recent proposals [16, 25].

Acknowledgments

We thank Prof. Hauke Lilie (Institute for Biochemistry and Biotechnology, Martin Luther University Halle-Wittenberg) for help with CD measurements and for discussion.

Statement of Ethics

An ethics statement was not required for this study type, since no humans or animal subjects or materials were used.

Conflict of Interest Statement

R. Gary Sawers was a member of the journal's Editorial Board at the time of submission. The other authors have no conflicts of interest to declare.

Funding Sources

This work received no specific grant from any funding agency and was supported financially by Martin Luther University, Halle (Saale) through funding by the state of Saxony-Anhalt. The funder had no role in the design, data collection, data analysis, and reporting of this study.

Author Contributions

Conceptualization, supervision, and writing: M.K. and R.G.S.; experimental analyses: O.T. and M.K.; data analysis: O.T., M.K., and R.G.S.; and reviewing and editing: R.G.S. All authors read and approved the final manuscript.

Data Availability Statement

The data that support the findings of this study are not publicly available due to privacy reasons but are available from the corresponding author (Gary Sawers) upon request.

References

1 Clarke DP. The fermentation pathways of *Escherichia coli*. FEMS Microbiol Rev. 1989; 63(3):223–34. https://doi.org/10.1016/0168-6445(89)90033-8

2 Kammel M, Erdmann C, Sawers RG. The formate-hydrogen axis and its impact on the physiology of enterobacterial fermentation. Adv Microb Physiol. 2024;84:51–82. https://doi.org/10.1016/bs.ampbs.2024.02.002

3 McDowall JS, Murphy BJ, Haumann M, Palmer T, Armstrong FA, Sargent F. Bacterial formate hydrogenlyase complex. Proc Natl Acad Sci USA. 2014;111(38):E3948–56. https://doi.org/10.1073/pnas.1407927111

4 Steinhilper R, Höff G, Heider J, Murphy BJ. Structure of the membrane-bound formate hydrogenlyase complex from *Escherichia coli*. Nat Commun. 2022;13(1):5395. https://doi.org/10.1038/s41467-022-32831-x

5 Peters K, Sargent F. Formate hydrogenlyase, formic acid translocation and hydrogen production: dynamic membrane biology during fermentation. Biochim Biophys Acta Bioenerg. 2023;1864(1):148919. https://doi.org/10.1016/j.bbabio.2022.148919

6 Hopper S, Böck A. Effector-mediated stimulation of ATPase activity by the sigma 54-dependent transcriptional activator FHLA from *Escherichia coli*. J Bacteriol. 1995; 177(10):2798–803. https://doi.org/10.1128/jb.177.10.2798-2803.1995

7 Rossmann R, Sawers G, Böck A. Mechanism of regulation of the formate-hydrogenlyase pathway by oxygen, nitrate and pH: definition of the formate regulon. Mol Microbiol. 1991;5(11):2807–14. https://doi.org/10.1111/j.1365-2958.1991.tb01989.x

8 Sauter M, Böhm R, Böck A. Mutational analysis of the operon (*hyc*) determining hydrogenase 3 formation in *Escherichia coli*. Mol Microbiol. 1992;6(11):1523–32. https://doi.org/10.1111/j.1365-2958.1992.tb00873.x

9 Lutz S, Jacobi A, Schlensog V, Böhm R, Sawers G, Böck A. Molecular characterization of an operon (*hyp*) necessary for the activity of the three hydrogenase isoenzymes in *Escherichia coli*. Mol Microbiol. 1991;5(1): 123–35. https://doi.org/10.1111/j.1365-2958.1991.tb01833.x

10 Zinoni F, Birkmann A, Stadtman TC, Böck A. Nucleotide sequence and expression of the selenocysteine-containing polypeptide of formate dehydrogenase (formate-hydrogenlyase-linked) from *Escherichia coli*. Proc Natl Acad Sci USA. 1986;83(13):4650–4. https://doi.org/10.1073/pnas.83.13.4650

11 Becker A, Fritz-Wolf K, Kabsch W, Knappe J, Schultz S, Volker Wagner AF. Structure and mechanism of the glycyl radical enzyme pyruvate formate-lyase. Nat Struct Biol. 1999;6(10):969–75. https://doi.org/10.1038/13341

12 Sawers G, Böck A. Novel transcriptional control of the pyruvate formate-lyase gene: upstream regulatory sequences and multiple promoters regulate anaerobic expression. J Bacteriol. 1989;171(5):2485–98. https://doi.org/10.1128/jb.171.5.2485-2498.1989

13 Suppmann B, Sawers G. Isolation and characterisation of hypophosphite-resistant mutants of *Escherichia coli*: identification of the FocA protein, encoded by the *pfl* operon, as a putative formate transporter. Mol Microbiol. 1994;11(5):965–82. https://doi.org/10.1111/j.1365-2958.1994.tb00375.x

14 Sawers RG. How FocA facilitates fermentation and respiration of formate by *Escherichia coli*. J Bacteriol. 2025;207(2):e0050224. https://doi.org/10.1128/jb.00502-24

15 Beyer L, Doberenz C, Falke D, Hunger D, Suppmann B, Sawers RG. Coordinating FocA and pyruvate formate-lyase synthesis in *Escherichia coli*: preferential translocation of formate over other mixed-acid fermentation products. J Bacteriol. 2013;195(7):1428–35. https://doi.org/10.1128/JB.02166-12

16 Metcalfe G, Sargent F, Hippler M. Hydrogen production in the presence of oxygen by *Escherichia coli* K-12. Microbiology. 2022;168(3):001167. https://doi.org/10.1099/mic.0.001167

17 Wang Y, Huang Y, Wang J, Cheng C, Huang W, Lu P, et al. Structure of the formate transporter FocA reveals a pentameric aquaporin-like channel. Nature. 2009;462(7272):467–72. https://doi.org/10.1038/nature08610

18 Lü W, Du J, Wacker T, Gerbig-Smentek E, Andrade SLA, Einsle O. pH-dependent gating in a FocA formate channel. Science. 2011;332(6027):352–4. https://doi.org/10.1126/science.1199098

19 Czyzewski BK, Wang DN. Identification and characterization of a bacterial hydrosulphide ion channel. Nature. 2012;483(7390):494–7. https://doi.org/10.1038/nature10881

20 Lü W, Schwarzer NJ, Du J, Gerbig-Smentek E, Andrade SLA, Einsle O. Structural and functional characterization of the nitrite channel NirC from *Salmonella* Typhimurium. Proc Nat Acad Sci USA. 2012;109(45):18395–400. https://doi.org/10.1073/pnas.1210793109

21 Kammel M, Trebbin O, Sawers RG. Interplay between the conserved pore residues Thr-91 and His-209 controls formate translocation through the FocA channel. Microb Physiol. 2022;32(3–4):95–107. https://doi.org/10.1159/000524454

22 Waight AB, Love J, Wang D-N. Structure and mechanism of a pentameric formate channel. Nat Struct Mol Biol. 2010;17(1):31–7. https://doi.org/10.1038/nsmb.1740

23 Kammel M, Trebbin O, Pinske C, Sawers RG. A single amino acid exchange converts FocA into a unidirectional efflux channel for formate. Microbiology. 2022;168(1):001132. https://doi.org/10.1099/mic.0.001132

24 Kammel M, Sawers RG. The FocA channel functions to maintain intracellular formate homeostasis during *Escherichia coli* fermentation. Microbiology. 2022;168(4). https://doi.org/10.1099/mic.0.001168

25 Kammel M, Pinske C, Sawers RG. FocA and its central role in fine-tuning pH homeostasis of enterobacterial formate metabolism. Microbiology. 2022;168(10). https://doi.org/10.1099/mic.0.001253

26 Broo KS, Brive L, Sott RS, Baltzer L. Site-selective control of the reactivity of surface-exposed histidine residues in designed four-helix-bundle catalysts. Fold Des. 1998;3(4):303–12. https://doi.org/10.1016/S1359-0278(98)00041-8

27 Poole LB. The basics of thiols and cysteines in redox biology and chemistry. Free Radic Biol Med. 2015;80:148–57. https://doi.org/10.1016/j.freeradbiomed.2014.11.013

28 Marino SM, Gladyshev VN. Analysis and functional prediction of reactive cysteine residues. J Biol Chem. 2012;287(7):4419–25. https://doi.org/10.1074/jbc.R111.275578

29 Kammel M, Hunger D, Sawers RG. The soluble cytoplasmic N-terminal domain of the FocA channel gates bidirectional formate translocation. Mol Microbiol. 2021;115(4):758–73. https://doi.org/10.1111/mmi.14641

30 Sambrook J, Fritsch EF, Maniatis T. Molecular cloning: a laboratory manual. 2nd ed. NY: Cold Spring Harbor; 1989.

31 Falke D, Schulz K, Doberenz C, Beyer L, Lilie H, Thiemer B, et al. Unexpected oligomeric structure of the FocA formate channel of *Escherichia coli*: a paradigm for the formate-nitrite transporter family of integral membrane proteins. FEMS Microbiol Lett. 2010;303(1):69–75. https://doi.org/10.1111/j.1574-6968.2009.01862.x

32 Hamilton CM, Aldea M, Washburn BK, Babitzke P, Kushner SR. New method for generating deletions and gene replacements in *Escherichia coli*. J Bacteriol. 1989;171(9):4617–22. https://doi.org/10.1128/jb.171.9.4617-4622.1989

33 Baba T, Ara T, Hasegawa M, Takai Y, Okumura Y, Baba M, et al. Construction of *Escherichia coli* K-12 in-frame, single-gene knockout mutants: the Keio collection. Mol Syst Biol. 2006;2(2):2006.0008. https://doi.org/10.1038/msb4100050

34 Miller J. Experiments in molecular genetics. NY: Cold Spring Harbor; 1972.

35 Cherepanov PP, Wackernagel W. Gene disruption in *Escherichia coli*: Tc^R and Km^R cassettes with the option of Flp-catalyzed excision of the antibiotic-resistance determinant. Gene. 1995;158(1):9–14. https://doi.org/10.1016/0378-1119(95)00193-a

36 Laemmli U. Cleavage of structural proteins during the assembly of the head of bacteriophage T4. Nature. 1970;227(5259):680–5. https://doi.org/10.1038/227680a0

37 Schägger H, von Jagow G. Blue native electrophoresis for isolation of membrane protein complexes in enzymatically active form. Anal Biochem. 1991;199(2):223–31. https://doi.org/10.1016/0003-2697(91)90094-a

38 Eisenberg D, Schwarz E, Komaromy M, Wall R. Analysis of membrane and surface protein sequences with the hydrophobic moment plot. J Mol Biol. 1984;179(1):125–42. https://doi.org/10.1016/0022-2836(84)90309-7

39 Hofer F, Kraml J, Kahler U, Kamenik AS, Liedl KR. Catalytic site p*Ka* values of aspartic, cysteine, and serine proteases: constant pH MD simulations. J Chem Inf Model. 2020;60(6):3030–42. https://doi.org/10.1021/acs.jcim.0c00190

40 Doberenz C, Zorn M, Falke D, Nannemann D, Hunger D, Beyer L, et al. Pyruvate formate-lyase interacts directly with the formate channel FocA to regulate formate translocation. J Mol Biol. 2014;426(15):2827–39. https://doi.org/10.1016/j.jmb.2014.05.023

41 Korsa I, Böck A. Characterization of *fhlA* mutations resulting in ligand-independent transcriptional activation and ATP hydrolysis. J Bacteriol. 1997;179(1):41–5. https://doi.org/10.1128/jb.179.1.41-45.1997

42 Mehler EL, Fuxreiter M, Simon I, Garcia-Moreno B. The role of hydrophobic microenvironments in modulating pKa shifts in proteins. Proteins. 2002;48(2):283–92. https://doi.org/10.1002/prot.10153

43 Vanyan L, Kammel M, Sawers RG, Trchounian K. Evidence for bidirectional formic acid translocation in vivo via the Escherichia coli formate channel FocA. Arch Biochem Biophys. 2024;752(2):109877. https://doi.org/10.1016/j.abb.2023.109877

44 Plaga W, Frank R, Knappe J. Catalytic-site mapping of pyruvate formate lyase: hypophosphite reaction on the acetyl-enzyme intermediate affords carbon-phosphorus bond synthesis (1-hydroxyethylphosphonate). Eur J Biochem. 1988;178(2):445–50. https://doi.org/10.1111/j.1432-1033.1988.tb14468.x

45 Maier A, Mguni LM, Ngo ACR, Tischler D. Formate dehydrogenase: recent developments for NADH and NADPH recycling in biocatalysis. ChemCatChem. 2024;16(21):e202401021. https://doi.org/10.1002/cctc.202401021

46 Sawers G. Specific transcriptional requirements for positive regulation of the anaerobically inducible *pfl* operon by ArcA and FNR. Mol Microbiol. 1993;10(4):737–47. https://doi.org/10.1111/j.1365-2958.1993.tb00944.x